A Quantitative Model of Technetium-99m-DTPA-Galactosyl-HSA for the Assessment of Hepatic Blood Flow and Hepatic Binding Receptor

Sang Kil Ha-Kawa and Yoshimasa Tanaka

Department of Radiology, Kansai Medical University, Moriguchi, Japan

Technetium-99m-diethylenetriaminepentaacetic acid-galactosyl-human serum albumin (^{99m}Tc-GSA) was studied in normal volunteers and in patients with impaired liver function. The extrapolation approach originated the absolute dose of ^{99m}Tc-GSA in blood and the hepatic blood volume. The heart and liver regression curves were simultaneously fractionated into the three compartments (extrahepatic blood, hepatic blood and hepatocytes). Four differential equations were integrated with the six parameters as variables, and the smallest residual sum of squares was obtained by the damping Gauss-Newton method. The result of hepatic blood flow was 1603 ± 144 (ml/min) in normal controls, which was compatible with previously reported values. Maximal removal rate (mg/min) showed statistically significant differences between the normal volunteers and patients with chronic hepatitis or liver cirrhosis. Our kinetic model of ^{99m}Tc-GSA can be used in the evaluation of liver function.

J Nucl Med 1991; 32:2233–2240

Ashwell and Morell demonstrated hepatic binding receptor for asialoglycoproteins with the investigation of ceruloplasmin metabolism (*1*). They found that ceruloplasmin molecules, which lack a sialic acid residue, rapidly disappeared from the circulation and were taken up by hepatocytes (*2*). This activity was found to be exclusively associated with a protein in the sinusoidal membrane of hepatocytes termed asialoglycoprotein receptor (*3*). This receptor decreases its number in patients with chronic liver diseases (*4*). Some investigators (*5–9*) labeled galactosyl-neoglycoalbumin with ^{99m}Tc for in vivo functional studies and imaging of the liver. Technetium-99m-diethylenetriaminepentaacetic acid-galactosyl-human serum albumin (GSA, Nihon Medi-Physics, Japan) is among the newly synthesized neoglycoalbumin for clinical hepatic imaging. Diethylenetriaminepentaacetic acid (DTPA) has been used for labeling natural glycoprotein, asialoorosomucoid, with technetium (*8,9*). Technetium-99m-GSA is a first neoglycoalbumin using DTPA for stable labeling. We investigated ^{99m}Tc-GSA in a human study. Model analysis for labeled neoglycoalbumin has been tested using a three-compartment model by Vera et al. (*10–12*) and a four-compartment model by Galli et al. (*9*). A good correlation was shown between the receptor population and the Child-Turcotte Criteria score (*12*) or other hepatic functional tests (*13*). However, their procedure requires blood sampling for dose calibration. We applied an extrapolation method to the heart and liver regression curves of ^{99m}Tc-GSA. This approach introduced the absolute time-dose curve of ^{99m}Tc-GSA in the blood, without blood sampling, and the blood volume in the liver. The purpose of this paper is to present a radiopharmacokinetic model of ^{99m}Tc-GSA for the assessment of hepatic blood flow (Q) and maximal removal rate (Rmax) by asialoglycoprotein in hepatocytes.

Received Dec. 21, 1990; revision accepted May 13, 1991.

For reprints contact: Sang Kil Ha-Kawa, MD, Department of Radiology, Kansai Medical University, 1, Fumizono-cho, Moriguchi, Osaka 570, Japan.

MATERIALS AND METHODS

Study Population

Four healthy volunteers constituted the normal control population. They ranged in age from 22 to 58 yr, with a mean of 32.0 ± 17.3 yr. None of them had a history of cardiac, renal, liver, or systemic illness. Routine blood biochemical data were normal for all of them. Laboratory tests performed 1, 7, and 30 days after the radioisotope study showed no appreciable changes. The diseased population consisted of 18 patients (9 males and 9 females), aged 22–71 yr (mean: 52.9 ± 14.5 yr), of whom seven had chronic hepatitis (CH), seven had compensated liver cirrhosis (CC), and four had decompensated liver cirrhosis (DC). All diagnoses were histologically confirmed, except for two patients with DC. None of the patients had a proven malignant lesion in the liver or any other organ.

Procedure

Unlabeled GSA, in kit form, was provided by Nihon Medi-Physics, Nishinomiya, Japan. The carbohydrate density was 36 galactose units per albumin molecule. Labeling could be achieved by addition of 2 ml/3.7 GBq of [^{99m}Tc]pertechnetate to the vial,

followed by 1 min of shaking. The radiochemical purity, determined by thin-layer chromatography, was greater than 98%.

All subjects received 1 mg/185 MBq (5m Ci) of ^{99m}Tc-GSA in 0.1 ml of saline, which was injected as a bolus dose into an antecubital vein. The radioactivity of the dose-containing syringe was measured in a dose calibrator before and after injection, for kinetic study.

Images were obtained using a large field of view gamma camera (Toshiba GCA-90B) equipped with a high-resolution, parallel-hole collimator, centered over the liver and precordium. Digital images were acquired into an on-line nuclear data processor (Toshiba GMS-55A) at 20-sec frames for the first 60 min after injection. At the end of the dynamic study, heparinized blood samples were removed from the contralateral vein. After the dynamic study, whole-body anterior images were obtained in the normal volunteers (n = 4). The counts of the liver and urine were compared with the whole-body counts for estimating percentage of the injected dose (%ID). The estimation of %ID in the liver and urine were obtained, instead of whole-body counts, from the known dose standard counts in 500 ml of saline in a flask under the same table-camera distance for each patient study. A calibration factor, obtained from the comparison of the liver-phantom and dose standard counts in a flask at the various distance between the table and gamma camera, was used for the attenuation correction. All counts were decay-corrected for ^{99m}Tc.

Blood Sample Scaling

The radioactivity of the blood samples and dose standards in 500 ml were measured in a well scintillation counter for calculating the %ID in blood. The total blood volume (TBV) was obtained from the following formulae;

$$TBV(L) = 0.1682 \times Height(m)^3 + 0.05048 \times Weight(kg) + 0.4444 \text{ for males}$$

$$TBV(L) = 0.2502 \times Height(m)^3 + 0.06253 \times Weight(kg) - 0.662 \text{ for females.}$$

Curve Generation

Curves were produced using regions of interest (ROIs) over the heart, whole liver and right middle-lung areas, avoiding the hilum. The lung curve, after correction for pixel numbers, was subtracted from the heart curve as background during the imaging time (0–60 min).

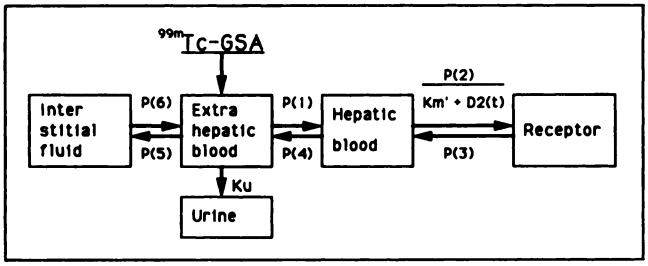

FIGURE 1. Compartmental scheme for the distribution of intravenously injected ^{99m}Tc-GSA. Compartment 1 is extrahepatic blood, Compartment 2 is hepatic blood, Compartment 3 is hepatocytes, Compartment 4 is interstitial fluid, and Compartment 5 is urine. The volume of the compartment was estimated only for extrahepatic blood (Ve) and hepatic blood (Vh) from Equations 12 and 13. Symbols are given in Table 1.

TABLE 1
Symbols

Symbol	Description	Units
D0	Injected dose of GSA	mg
D1(t)	GSA in extrahepatic blood (at t min after injection)	mg
D2(t)	GSA in hepatic blood (at t min after injection)	mg
D3(t)	GSA in hepatocytes (at t min after injection)	mg
D4(t)	GSA in interstitial fluid (at t min after injection)	mg
D5(t)	GSA in urine (at t min after injection)	mg
Ve	Extrahepatic blood volume	ml
Vh	Hepatic blood volume	ml
Ku	Urinary elimination rate constant	min^{-1}
Km'	Volume-corrected Michaelis constant	mg
Q	Hepatic blood flow	ml/min
Rmax	Maximal removal rate	mg/min
Estimated variable parameter		
P(1)	Inflow rate to liver (=Q/Ve)	min^{-1}
P(2)	Maximal removal rate (Rmax)	mg/min
P(3)	Reverse binding rate	min^{-1}
P(4)	Outflow rate from liver (=Q/Vh)	min^{-1}
P(5)	Diffusion rate from blood to interstitial fluid	min^{-1}
P(6)	Backdiffusion rate from interstitial fluid to blood	min^{-1}

Description of Heart and Liver Curve as the Sum of Biexponential Functions

The biexponential functions:

$$y(t) = A_1e^{-k1t} + A_2e^{-k2t}$$

were fitted to the heart and liver data from 2 to 60 min using a non-linear least-squares fitting routine. Early data from 0 to 2 min after injection were excluded from the fit since that was regarded as the initial distribution phase. A multiple correlation coefficient was provided as an index of approximation between the regression and observed data.

Kinetic Model

The general structure of this model was composed of five compartments for describing ^{99m}Tc-GSA: (1) extrahepatic blood, (2) hepatic blood, (3) hepatocytes, (4) interstitial fluid and (5) urine (Fig. 1). The symbols are given in Table 1.

Data Processing

Based on the biexponential regression curve, the following assumptions are introduced.

1. The background-subtracted heart regression curve from 2 to 60 min represents the uniformly distributed ^{99m}Tc-GSA in the extrahepatic compartment (C1) and hepatic blood compartment (C2). Ligand concentration in C1 alters with equal concentration in C2.
2. Extrapolation to time 0 on the heart regression curve also represents the uniform distribution and same concentration of ligand in both blood compartments (C1 and C2) from 0 to 2 min. Y-intercept of the heart regression curve (time 0) reflects the total injected dose of ^{99m}Tc-GSA. This conception means any amount of ^{99m}Tc-GSA is not delivered to the hepatocytes compartment (C3), interstitial fluid compartment (C4) and urine compartment (C5) at time 0.
3. The liver regression curve extrapolated to time 0 represents the sum of ligand in C2 and C3 from 0 to 60 min.
4. Y-intercept of the liver regression curve reflects the amount of the ligand in C2 alone.

5. From items 1 and 2, C1 and C2 have the same ligand concentration at any time from 0 to 60 min, hence, D2(t)/(D1(t) + D2(t)) is a constant value that always depends on the volume ratio of Vh/TBV.
6. The sum of the whole compartmental dose (D1(t) + D2(t) + D3(t) + D4(t) + D5(t), mg) is equal to the injected dose (D0, mg). It is assumed that D1(t) and D3(t) are detected with equal efficiency.

Thus, the heart and liver regression curves related to D1(t), D2(t), and D3(t) are as follows (time = t, $0 \leqq t \leqq 60$):

$$HD(t) = D1(t) + D2(t) \quad \text{Eq. 1}$$

$$LD(t) = D2(t) + D3(t), \quad \text{Eq. 2}$$

where HD(t) is the heart regression curve and LD(t) is the liver regression curve both expressed as a unit of mg of GSA. Data conversion from counts per minute to milligrams were performed as follows: HD(t) was obtained by the normalization of the y-intercept of the heart regression from assumption 2; and LD(t) was obtained from a comparison of the whole-body counts or dose standard counts with the liver counts at 60 min after infection. Attenuation correction was performed using the value of fc (mean: 1.46) between ROI data and dose standards.

From assumptions 3 and 4,

$$D3(0) = 0, \quad \text{Eq. 3}$$

which yields

$$LD(0) = D2(0). \quad \text{Eq. 4}$$

Equation 4 was substituted into Equation 1 and

$$D1(0) = HD(0) - LD(0) \quad \text{Eq. 5}$$

was obtained.

From assumption 5 and Equation 4,

$$\frac{D2(t)}{D1(t) + D2(t)} = \frac{D2(0)}{D1(0) + D2(0)} = \frac{LD(0)}{HD(0)} \quad \text{Eq. 6}$$

was obtained. Equation 1 was substituted into Equation 6 yielding

$$D2(t) = HD(t) \times (LD(0)/HD(0)), \quad \text{Eq. 7}$$

and hence

$$D1(t) = HD(t) \times (1 - LD(0)/HD(0)) \quad \text{Eq. 8}$$

$$D3(t) = LD(t) - HD(t) \times (LD(0)/HD(0)), \quad \text{Eq. 9}$$

were obtained. Since HD(0) and LD(0) were known values from the extrapolation of the heart and liver regression curves, D1(t), D2(t) and D3(t) were decided absolutely for 60 min.

Ku and D5(t) were obtained as follows:

$$Ku = UD(60) \Big/ \int_0^{60} D1(t)dt \quad \text{Eq. 10}$$

$$D5(t) = Ku \times \int_0^t D1(t)dt, \quad \text{Eq. 11}$$

where UD(60) (mg) is the cumulative urinary dose for 60 min, which is obtained from the counts in the urinary bladder at 60 min after injection. From assumption 6, D4(t) was the remainder of D0 after the subtraction of the sum of the dose in the other compartments. Thus, we obtained the independent time-course data each of the five compartments as unit of mg of ^{99m}Tc-GSA.

From assumption 5 and Equation 1, TBV was fractionated into the volume of extrahepatic and hepatic blood as follows:

$$Vh = TBV \times (D2(0)/HD(0))) \quad \text{Eq. 12}$$

$$Ve = TBV - Vh. \quad \text{Eq. 13}$$

Km′ was calculated according to the equation:

$$Km' = 1.239 \times Vh \times 10^{-3}. \quad \text{Eq. 14}$$

We obtained a value of 1.239×10^{-3} (mg/liter) as the Michaelis constant of ^{99m}Tc-GSA from the supplementary study (see Results). The model, therefore, was described by the following mass-balance equations:

$$\frac{dD1}{dt} = -(P(1) + P(5) + Ku) \times D1 + P(4) \times D2 + P(6) \times D4 \quad \text{Eq. 15}$$

$$\frac{dD2}{dt} = -\left(\frac{P(2)}{Km' + D2} + P(4)\right) \times D2 + P(1) \times D1 + P(3) \times D3 \quad \text{Eq. 16}$$

$$\frac{dD3}{dt} = -P(3) \times D3 + \frac{P(2) \times D2}{Km' + D2} \quad \text{Eq. 17}$$

$$\frac{dD4}{dt} = -P(6) \times D4 + P(5) \times D1 \quad \text{Eq. 18}$$

under initial conditions of

$$D1(0) = HD(0) - LD(0) \quad \text{Eq. 19}$$

$$D2(0) = LD(0) \quad \text{Eq. 20}$$

$$D3(0) = 0 \quad \text{Eq. 21}$$

$$D4(0) = 0. \quad \text{Eq. 22}$$

Computer Algorithms

Equations 15–18 were nonlinear, and it was difficult to obtain analytical solutions. These equations were integrated numerically using a fourth-order Runge-Kutta-Gill scheme (*14*) with the six parameters as variables. Residual sum of squares for the four-compartmental data set was obtained for any given set of parameters. Iterative minimisation of the residual sum of squares was obtained by varying the six parameters set using the damping Gauss-Newton method (*14*), which is a nonlinear least-squares algorithm. We placed each 1-min values from 1 to 30 min of D1(t) – D4(t) (total of 120 points) as non-weighted input data. The initial values of six variable parameters at the start of calculation were as follows: P(1) = (0.03, 0.05, 0.1, 0.25, 0.35, and 0.5), P(2) = (0.01, 0.03, 0.1, 0.15, 0.2, and 0.5), P(3) = 0.03, P(4) = 2.0, P(5) = 0.1, P(6) = 0.1. The final set of six parameters was determined by the smallest residual sum of squares for the total compartmental data set. The Q was obtained from the final P(1) × Ve and the Rmax was equal to the final P(2).

Statistical Analysis

A multiple correlation coefficient (R) was calculated as an index of the goodness of biexponential regression for the heart and liver time-activity curve. The significance of R was determined using F statistics. Group results are given as means ±

TABLE 2
Results of Supplementary Multi-Dose Study for Michaelis-Menten Kinetics in Normal Volunteers (n = 5)

Patient no.	D0* (mg)	D2(0)†/D0	Vh‡ (ml)	S/Vh§ (mg/l)	R¶ (mg/min)
1	1	0.136	591	0.213	0.0983
2	1	0.124	626	0.181	0.0833
3	1	0.138	549	0.234	0.0863
4	5	0.161	742	1.040	0.2429
5	10	0.170	680	2.357	0.6012

* Injected dose of ^{99m}Tc-GSA.

† Initial dose of ^{99m}Tc-GSA in the hepatic blood and ‡ hepatic blood volume are obtained from extrapolation of the liver regression curve (see text for details).

§ Initial concentration and ¶initial removal rate of ^{99m}Tc-GSA. S is obtained from (D2(0)+D2(1))/2 and R is obtained from D3(1) (see text for details).

standard deviation. The significance of differences between the control and patient groups was determined using Student's paired t-test. A p value of less than 0.05 was considered significant.

RESULTS

Table 2 shows the supplementary multi-dose study in five normal volunteers. Initial removal rates in high dose subjects are not proportional to the initial concentration. This finding suggests a saturation kinetics of ^{99m}Tc-GSA, consistent with the Michaelis-Menten relation. Their reciprocal values are plotted in Figure 2 (Lineweaver-Burk plot). The absolute reciprocal of the x-intercept of the linear regression line ($y = 1.605 + 1.988 \times$) is the Michaelis constant (1.239 mg/liter). The reciprocal of the y-intercept (0.623 mg/min) is the maximal removal rate (Rmax) by the plot method.

Table 3 gives the patient characteristics, %ID in the liver and urine at 60 min after injection, and the multiple correlation coefficient and its F statistics for the heart and liver regression curves. The %ID in the liver at 60 min after injection was 59.6% ± 2.5% in the NC group. There were significant differences between the NC group and with the CH (43.0% ± 10.6%, $p < 0.05$), CC (21.7% ± 8.0%, $p < 0.001$) and DC groups (21.8% ± 15.9%, $p < 0.01$). Biexponential regression of the heart and liver time-activity curves both showed significant goodness of fit ($p < 0.001$) in all subjects. A representative observed data and the regression curves of the heart and liver for Patient 20 are illustrated in Figure 3.

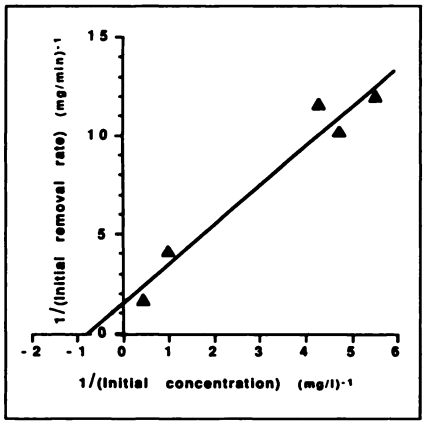

FIGURE 2. Lineweaver-Burk plot (double reciprocal plot) from normal volunteers (n = 5) for estimating the Michaelis constant. Data value are shown in Table 2. The abscissa is the reciprocal of the initial concentration of ^{99m}Tc-GSA in the hepatic blood, while the ordinate is the reciprocal of the initial removal dose by the receptors.

The results of parameter estimates are shown in Table 4. LD(0)/D0 values were 0.143 ± 0.022 in the NC group, and 0.158 ± 0.030 in the CH, 0.009 ± 0.034 in the CC, and 0.095 ± 0.035 in the DC groups, respectively. The result in the CC group was significantly lower than that in the NC group ($p < 0.05$).

The %ID from the heart regression curve at 60 min after injection is highly correlated ($r = 0.926$) with the %ID from the blood samples (Fig. 4). The differences between the %ID from the regression curve and blood samples in each subject were 4.1% ± 4.1%.

A representative example of the compartmental dose curve from D1(t) to D5(t) is shown in Figure 5. Figure 6 illustrates the standardized residuals between the heart or liver time-activity curve and the resulting theoretical curve after the computing calculation.

The Q values were 1603 ± 144 ml/min in the NC group, and 1265 ± 310 ml/min in the CH, 905 ± 378 ml/min in the CC and 626 ± 213 ml/min in the DC groups. There is no significant difference in Q between the NC and CH groups, whereas it is significantly decreased in the CC ($p < 0.01$) or in the DC ($p < 0.001$) group (Fig. 7).

The Rmax values were 0.509 ± 0.095 mg/min in the NC group, and 0.327 ± 0.118 mg/min ($p < 0.05$) in the CH, 0.009 ± 0.07 mg/min ($p < 0.001$) in CC and 0.054 ± 0.028 mg/min ($p < 0.001$) in DC groups. The Rmax is significantly different between the NC group and each patient group (Fig. 8). There are also differences between the CH and CC ($p < 0.001$) group and between the CH and DC ($p < 0.01$) group.

DISCUSSION

In 1984, Vera et al. (*10*) proposed a kinetic model for ^{99m}Tc-GSA. Their model is of theoretic value for estimating blood flow, receptor concentration and receptor-ligand affinity. However, it requires blood samples for units conversion from cpm to molar dose of ligand. Our ^{99m}Tc-GSA model can be clearly distinguished from theirs by the following three points. First, we take an extrapolating approach to the heart time-activity curve to obtain a calibration coefficient for calculating the amount of ^{99m}Tc-GSA in the blood. Second, the same approach to the liver time-activity curve makes it possible to estimate hepatic blood volume. Finally, Michaelis-Menten-type kinetics are applied to receptor-ligand binding (*15*): this approach provides a dose-independent index for the amount of receptors.

TABLE 3
Patients Characteristics, %Dose of Liver and Urine, and Results of Biexponential Fit

Patient no.	Age/ Sex	%ID*		Heart		Liver	
		Liver	Urine	R†	F-value‡	R†	F-value‡
Normal control (n = 4)							
1	22/M	56.5	9.2	0.991	958	0.994	1589
2	23/M	58.7	5.9	0.955	188	0.998	4113
3	23/M	61.6	4.6	0.993	1313	0.998	2789
4	58/M	61.5	4.4	0.976	364	0.992	1168
Chronic hepatitis (n = 7)							
5	48/M	50.8	17.4	0.984	555	0.998	3675
6	40/M	28.0	9.4	0.922	103	0.986	627
7	68/F	50.2	11.1	0.981	468	0.999	8885
8	36/M	51.8	8.9	0.987	669	0.999	11678
9	22/M	50.8	12.9	0.964	238	0.998	4119
10	30/M	40.0	12.3	0.981	460	0.999	6325
11	71/F	29.1	8.4	0.974	339	0.999	7158
Compensated cirrhosis (n = 7)							
12	62/F	24.8	11.1	0.980	455	0.998	4008
13	60/F	12.4	12.0	0.908	86	0.994	1548
14	66/M	27.6	6.3	0.953	182	0.999	7192
15	57/F	23.8	6.5	0.974	335	0.999	9080
16	68/F	13.4	12.1	0.980	439	0.994	1552
17	40/M	33.9	8.7	0.979	423	0.998	3836
18	63/M	15.8	5.1	0.945	154	0.999	7396
Decompensated cirrhosis (n = 4)							
19	60/F	15.9	14.1	0.962	229	0.998	3632
20	61/F	41.6	2.3	0.994	1465	0.999	12647
21	65/F	25.7	4.8	0.973	323	0.999	10695
22	41/M	3.9	4.5	0.883	65	0.802	33

* Calculated from counts of ROI at 60 min after injection.
† Multiple correlation coefficient between observed data and regression curve from 2 to 60 min (59 points) after injection.
‡ $P(F(3,55) > 6.25) < 0.001$.

We assumed that uniform distribution of ^{99m}Tc-GSA in the blood space is achieved within 2 min after injection. The heart curve decreases from 2 min after injection because of the shift of ligand from the blood compartments (C1 and C2) to the other compartments (C3, C4, and C5). However, the radioactivity in the heart ROI at 2 min after injection could not be regarded as total radioactivity of the injected ^{99m}Tc-GSA, since ligand-receptor binding has already proceeded by 2 min. We postulate that the y-intercept of the heart regression curve means a distribution of ligand confined to C1 and C2 alone, not included to the other compartments. This conception yields a calibration coefficient to estimate the ligand dose in the blood. Thus, without blood sampling, we were able to determine the ligand dose as a unit of mg in the blood compartments (D1(t) and D2(t)) at any time for 60 min. The %ID from regression curve was comparable to the result from blood samples. This fact endorsed the validity of our extrapolation approach.

The liver ROI includes the activity of the ligand both in the hepatic blood and hepatocytes. The proportion of the hepatic blood volume to the total blood volume is known to be 14% at a physiologic level in normal health (*16*). We obtained similar results that are reflected in the value of LD(0)/D0 in normal subjects. This ratio is probably not a constant value. In fibrosis and cirrhosis, capillarization of sinusoids (*17*) leads to a reduction of the hepatic vascular volume. Our observation that LD(0)/D0 was significantly decreased in the patients with cirrhosis is in good agreement with this finding. The mean Q value in the normal group determined with our model is 1603 ± 144 ml/min, which is in accordance with the reported findings in healthy normal humans (*18*). Although this study was not designed to verify hepatic blood flow in cirrhotic patients, it is intriguing that Q was significantly lower in the CC and DC groups than in the normal group.

One of the features in receptor-binding kinetics is a limitation of its binding capacity. We therefore adopted a nonlinear parameter of Michaelis-Menten-type kinetics for the binding process. Our supplementary multi-dose study showed saturation uptake of ^{99m}Tc-GSA in normal volunteers. Saturation uptake was observed in the in vitro study for asialoorosomucoid (*19,20*), and Michaelis-Menten kinetics were accepted in the in vivo study (*15*). The

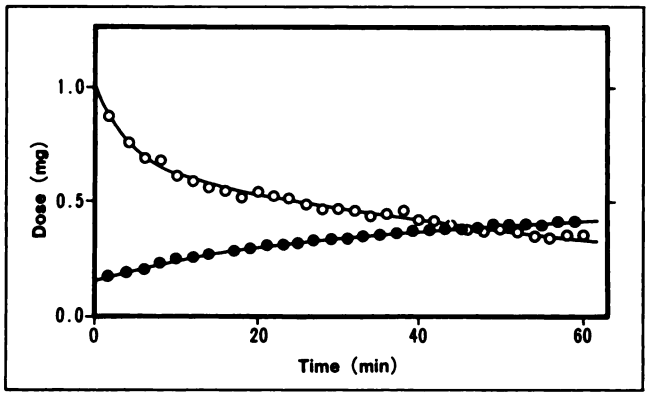

FIGURE 3. Representative background-subtracted heart (○) and liver (●) plots for ^{99m}Tc-GSA in Patient 20. The even-minute data are plotted from 2 to 60 min after injection. Regression curves are expressed by solid lines. The extrapolated y-intercept (time = 0) of the heart regression curve is assumed to be equivalent to the total injected dose. The extrapolated y-intercept (time = 0) of the liver regression curve is assumed to be equivalent to the amount of ^{99m}Tc-GSA in the hepatic blood.

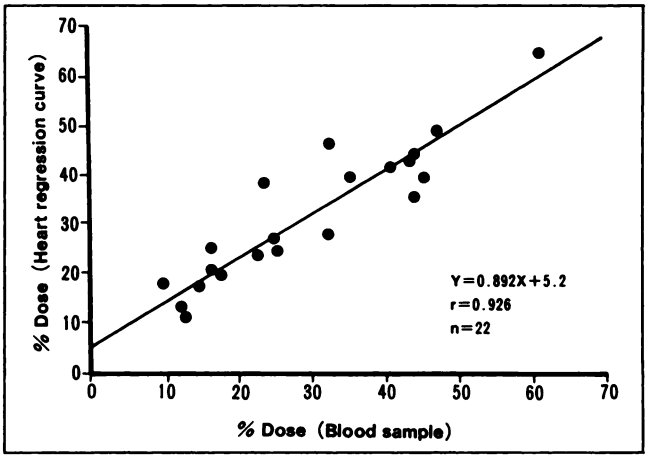

FIGURE 4. Comparison of the %ID in the blood at 60 min after injection estimated from the extrapolated heart regression curve and by the direct measurement of the blood samples. The value of the heart regression curve is expressed as the % of counts on the y-intercept (time = 0). The results of regression analysis are in good agreement with the findings of blood samples.

saturation kinetics is described as P(2)/(Km′ + D2(t)) in this model. P(2) therein means the maximum rate of removal of the ligand per min from the hepatic vascular space to the receptors in the sinusoidal membrane of hepatocytes. The Rmax decreased with the severity of liver disease. There was also a significant difference in the Rmax between the CH and normal group, which indicates a high sensitivity of this analysis. A mean time of 15.9 min is required to recycle an unoccupied surface receptor (*21*).

TABLE 4
Results of Parameter Estimates

Patient no.	Fixed Parameters				Variable Parameters						
	LD(0)/D0	Vh (ml)	Km′ (mg)	Ku*	p(1) (min^{-1})	p(2) (mg/min)	p(3) (min^{-1})	p(4) (min^{-1})	p(5) (min^{-1})	p(6) (min^{-1})	CV‡ (%)
1	0.136	591	0.732	6.78	0.440 (7.0)†	0.551 (5.7)	0.061 (1.9)	1.780 (0.4)	0.062 (1.7)	0.051 (2.3)	2.30
2	0.124	626	0.776	3.70	0.405 (5.2)	0.614 (4.3)	0.059 (2.0)	1.763 (0.6)	0.113 (1.6)	0.137 (1.8)	2.20
3	0.138	549	0.680	3.43	0.442 (9.2)	0.477 (7.5)	0.056 (2.0)	1.839 (0.3)	0.044 (2.2)	0.068 (2.5)	2.00
4	0.175	789	0.977	3.03	0.393 (7.5)	0.394 (7.4)	0.027 (0.3)	2.016 (0.3)	0.059 (1.2)	0.018 (1.5)	0.89
5	0.206	945	1.170	9.21	0.490 (1.1)	0.458 (1.3)	0.065 (0.9)	1.933 (0.3)	0.091 (0.8)	0.176 (0.9)	1.09
6	0.124	704	0.872	4.12	0.295 (5.2)	0.230 (5.4)	0.048 (1.3)	2.233 (0.5)	0.037 (0.8)	0.027 (1.4)	0.94
7	0.170	533	0.661	6.25	0.363 (8.9)	0.326 (9.1)	0.048 (2.1)	2.005 (0.4)	0.044 (1.3)	0.049 (1.2)	1.17
8	0.164	709	0.878	4.87	0.377 (6.8)	0.366 (6.8)	0.040 (2.4)	2.038 (0.3)	0.061 (1.5)	0.090 (1.6)	1.88
9	0.173	658	0.818	8.26	0.378 (4.6)	0.480 (4.9)	0.053 (2.3)	0.883 (0.4)	0.885 (1.4)	0.105 (1.7)	2.09
10	0.150	653	0.809	5.67	0.330 (9.1)	0.277 (9.3)	0.044 (1.6)	2.152 (0.1)	0.027 (1.2)	0.024 (1.7)	0.79
11	0.122	406	0.504	3.91	0.302 (2.8)	0.154 (3.0)	0.052 (1.7)	2.119 (0.5)	0.097 (0.7)	0.085 (0.8)	1.39
12	0.109	428	0.530	4.08	0.277 (1.1)	0.102 (1.0)	0.043 (0.6)	2.326 (0.2)	0.068 (0.2)	0.085 (0.2)	0.34
13	0.086	266	0.329	3.99	0.208 (5.4)	0.061 (5.8)	0.110 (4.9)	2.412 (0.3)	0.152 (1.8)	0.229 (2.0)	2.73
14	0.112	526	0.652	1.83	0.272 (17.4)	0.109 (17.1)	0.046 (9.0)	2.366 (0.9)	0.065 (5.1)	0.249 (5.3)	4.20
15	0.099	334	0.414	2.14	0.261 (7.2)	0.069 (6.7)	0.037 (3.7)	2.380 (1.1)	0.057 (1.2)	0.100 (1.3)	1.75
16	0.088	284	0.352	3.89	0.230 (3.0)	0.042 (2.7)	0.060 (1.7)	2.440 (0.3)	0.065 (0.5)	0.095 (0.6)	0.82
17	0.157	767	0.950	4.26	0.393 (2.0)	0.248 (2.7)	0.050 (2.1)	2.125 (1.1)	0.076 (0.9)	0.069 (1.3)	1.77
18	0.045	222	0.275	1.83	0.117 (2.7)	0.059 (2.4)	0.013 (1.9)	2.468 (0.2)	0.072 (0.2)	0.054 (0.2)	0.28
19	0.083	265	0.328	4.28	0.199 (4.2)	0.041 (4.0)	0.037 (1.6)	2.475 (0.1)	0.042 (0.4)	0.078 (0.5)	0.63
20	0.147	354	0.439	0.77	0.343 (11.9)	0.082 (11.5)	0.030 (2.3)	2.302 (0.9)	0.035 (1.8)	0.103 (1.1)	1.03
21	0.072	166	0.205	1.63	0.166 (10.5)	0.072 (10.2)	0.027 (2.3)	2.400 (0.4)	0.051 (0.8)	0.085 (0.6)	0.88
22	0.076	309	0.382	2.01	0.228 (10.1)	0.021 (8.6)	0.111 (5.2)	2.509 (0.8)	0.033 (1.6)	0.116 (1.8)	1.76

LD(0) = initial dose in hepatic blood estimated from liver regression curve and D0 = total injected dose.
* Urinary elimination rate constant, $\times 10^{-3}$ (min^{-1}).
† Coefficient of variation (%) for each variable parameter in parentheses.
‡ Coefficient of variation (%) for total residual error (n = 120).

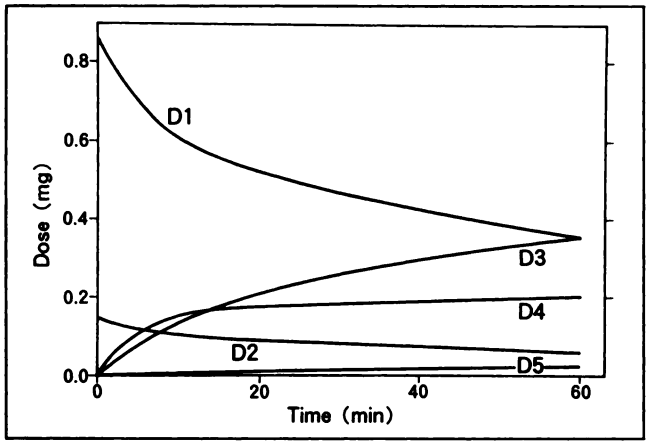

FIGURE 5. An example of the compartmental dose curve (D1(t)-D5(t)) derived from Patient 20 60 min after injection. The data are expressed as mg of ^{99m}Tc-GSA.

The Rmax shown in this paper would represent both initial and recycled number of receptors since we selected the first 30 min as a computing time. We did not take into account the elimination of radioactivity to the bile because its appearance in the bile ducts or gallbladder was faint and usually occurred later than 40 min after injection.

There are unsolved problems concerning the physiologic significance of P(3), P(5) and P(6). The most impaired patient (no. 22) showed relatively high values for P(3), suggesting early release of the bound label in severely impaired liver.

This model provides a noninvasive (bloodless) approach for estimating both hepatic blood flow and receptor population. Our future task will be to clarify:

1. Whether data provided by this model are useful for determining prognosis and for ascertaining patient response to various treatments.
2. Whether these data can serve as criteria for selecting surgical candidates.

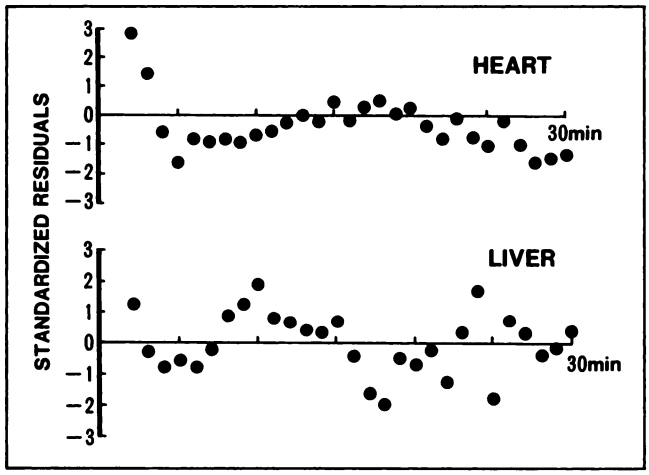

FIGURE 6. Standardized residuals between the heart or liver time-activity curve and its theoretical curve in a patient No. 20. The abscissa for the heart (upper side) is derived from the theoretical results of D1 + D2. The abscissa for the liver (lower side) is derived from the theoretical results of D2 + D3.

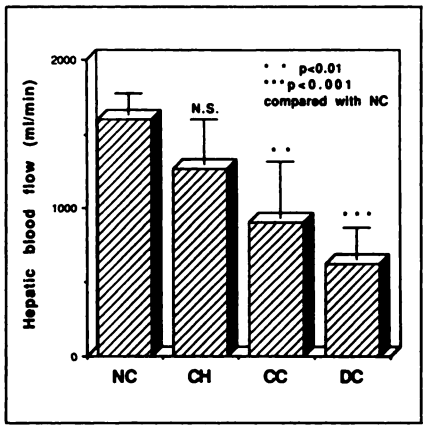

FIGURE 7. Comparison of the hepatic blood flow (ml/min, obtained from multiplying the final P(1) by the extrahepatic blood volume), in the normal control group (NC) and various liver disease groups (CH: chronic hepatitis; CC: compensated cirrhosis; DC: decompensated cirrhosis). compensated cirrhosis).

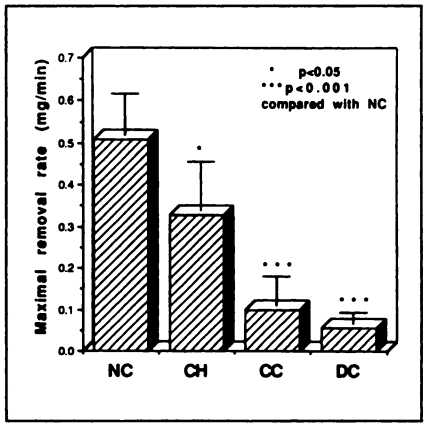

FIGURE 8. Comparison of the maximal removal rate (mg/min, obtained from the final P(2)), in the normal control group (NC) and the various liver disease groups (CH: chronic hepatitis; CC: compensated cirrhosis; DC: decompensated cirrhosis).

ACKNOWLEDGMENTS

The authors thank Shin-ichi Kitagawa, MD and Yoshitugu Kubota, MD for referring patients for this study and Yutaka Suga and other members of the Division of Nuclear Medicine for their excellent technical assistance. They also thank Nihon Medi-Physics Co., Ltd, (Nishinomiya, Japan) for their generous supply of ^{99m}Tc generator and diethylenetriaminepentaacetic acid-galactosyl-human serum albumin.

REFERENCES

1. Morell AG, Irvine RA, Sternlieb I, Scheunberg IH, Ashwell G. Physical and chemical studies on ceruloplasmin. V. Metabolic studies on sialic acid free ceruloplasmin in vivo. *J Biol Chem* 1968;243:155–159.
2. Pricer WE, Ashwell G. The binding of desialylated glycoproteins by plasma membranes of liver. *J Biol Chem* 1971;246:4825–4833.
3. Ashwell G, Morell AG. The role of surface carbohydrates in the hepatic recognition and transport of circulating glycoproteins. *Adv Enzymol* 1974;41:99–128.
4. Sawamura T, Nakada H, Hazama H, et al. Hyperasialoglycoproteinemia in patients with chronic liver diseases and/or liver cell carcinoma. *Gastroenterology* 1984;87:1217–1221.
5. van Rijk PP, van den Hamer CJA. Labelled asialo-orosomucoid in liver function studies. *Nuklearmedizin* 1977;14(suppl 1):570–572.
6. Krohn KA, Vera DR, Steffen SM. [^{99m}Tc]-Neogalactoalbumin: a general model for some bifunctional carbohydrates. *J Lab Comp Radiopharm* 1980;18:91–93.

7. Kawa S, Hazama H, Kojima M, et al. A new liver function test using the asialoglycoprotein-receptor system on the liver cell membrane. 2. Quantitative evaluation of labeled neoglycoprotein clearance. *Jpn J Nucl Med* 1986;23:907–916.
8. Galli G, Maini CL, Orlando P, Deleide G, Valle G. A radiopharmaceutical for the study of the liver: ^{99m}Tc-DTPA-asialo-orosomucoid. 1. Radiochemical and animal distribution studies. *J Nucl Med Allied Sci* 1988;32:109–116.
9. Galli G, Maini CL, Orlando P, Cobelli C, Thomaset K. A radiopharmaceutical for the study of the liver: ^{99m}Tc-DTPA-asialo-orosomucoid. 2. Human dynamic and imaging studies. *J Nucl Med Allied Sci* 1988;32:117–126.
10. Vera DR, Krohn KA, Stadalnik RC, Sceibe PO. Tc-99m-galactosyl-neoglycoalbumin: in vitro characterization of receptor-mediated binding. *J Nucl Med* 1984;25:779–787.
11. Vera DR, Krohn KA, Scheibe PO, Stadalnik RC. Identifiability analysis of an in vivo receptor-binding radiopharmacokinetic system. *IEEE Trans Biomed Eng* 1985;BME-32,312–322.
12. Stadalnik RC, Vera DR, Woodle S, et al. Technetium-99m-NGA functional hepatic imaging: preliminary clinical experience. *J Nucl Med* 1985;26:1233–1242.
13. Kudo M, Vera DR, Stadalnik RC, Trudeau WL, Ikekubo K, Todo A. In vivo estimates of hepatic binding protein concentration: correlation with classical indicators of hepatic functional reserve. *Am J Gastroenterol* 1990;85:1142–1148.
14. Yamaoka K, Nakagawa T. A nonlinear least squares program based on differential equations, MULTI(RUNGE), for microcomputers. *J Pharmacobiodyn* 1983;6:595–606.
15. Appel M, Potrat P, Feger J, Mas-Chamberlin C, Durand G. In vivo quantification of removal of asilo-orosomucoid from the circulation in anaesthetized streptozotocin-diabetic rats. *Diabetologia* 1986;29:383–387.
16. Lautt WW. Hepatic vasculature: a conceptual review. *Gastroenterology* 1977;73:1163–1169.
17. Schaffner F, Popper H. Capillarization of hepatic sinusoids in man. *Gastroenterology* 1963;44:239–242.
18. Bradley SE, Ingelfinger FJ, Bradley GP, Curry JJ. Estimation of hepatic blood flow in man. *J Clin Invest* 1945;24:890–897.
19. Weigel PH. Characterization of the asialoglycoprotein receptor on isolated rat hepatocytes. *J Biol Chem* 1980;255:6111–6120.
20. Dodeur M, Durand D, Dumont J, Durand G, Feger J, Agneray J. Effects of streptozotocin-induced diabetes mellitus on the binding and uptake of asialoorosomucoid by isolated hepatocytes from rats. *Eur J Biochem* 1982;123:383–387.
21. Schwartz AL, Fridovich SE, Lodish HF. Kinetics of internalization and recycling of the asialoglycoprotein receptor in a hepatoma cell line. *J Biol Chem* 1982;257:4230.